THE CRACK OPENING DISPLACEMENT OF ROCK FRACTURE PROCESS ZONE

by

Sheng ZHANG [a,b]*, Yang QIAO [a], and Hong-Bao ZHAO [c]

[a] School of Energy Science and Engineering, Henan Polytechnic University, Henan, China
[b] Collaborative Innovation Center of Coal Work Safety, Henan, China
[c] School of Resources and Safety Engineering,
China University of Mining and Technology, Beijing, China

Original scientific paper
https://doi.org/10.2298/TSCI180913214Z

The original displacement value of fracture process zone can be obtained by digital image correlation technology. According to the virtual crack model, the formula to obtain the opening displacement is given in the experiment. Basing on the damage Mechanics theory and the actual deformation characteristics of fracture process zone, the traditional opening displacement distribution function of fracture process zone is modified by defining the wave coefficient and the damage factor of the horizontal elastic modulus. The measured opening displacement is compared with the opening displacement of the traditional theoretical function and modified function, and the results show that the opening displacement is non-linear fluctuation characteristic distribution influenced by damage. The revise distribution function not only reflects the overall growth trend of the opening displacement, but also reflects the local fluctuation characteristics. It has an important theoretical significance for understanding the non-linear characteristics of rock fracture process.

Key words: *virtual crack, opening displacement, fracture process zone, damage factor, fluctuation coefficient*

Introduction

The fracture process zone (FPZ) of quasi-brittle material has always been a hot issue for scholars, because it is the key to solve the size effect of rock fracture toughness and the non-linear phenomena. The virtual crack model has been always a usual study model. Constitutive relation and deformation state of virtual crack has been described by two physical parameters, one is the cohesion, and the other is the opening displacement. Because of the distribution characteristics and properties of the cohesion, it is difficult to directly measure the cohesion in the experiment. Therefore, the opening displacement has been a key factor to study the characteristics of the FPZ.

The digital image correlation (DIC) technology has been used to obtain the full-field displacement data of the specimen, see [1, 2]. By extracting the horizontal displacement of the sampling line on both sides of the pre-crack and subtracting it, the opening displacement at different loading stages and the ultimate opening displacement was obtained. Ji *et al*. [3] simply used the experimental method to obtain the opening displacement of sandstone specimen [3]. The variation trend of the opening displacement inside FPZ was analyzed, and it was found that the front end of FPZ was the deformation change point of the fracture ligament [4]. The

* Corresponding author, e-mail: zhangs@hpu.edu.cn

relationships between FPZ and the fracture toughness and tensile strength were derived by the relationship between the opening displacement and the stress at different angles of the crack tip [5]. Based on the virtual crack model and combined with the bilinear tensile softening curve, the distribution of opening displacement of FPZ was revealed [6]. According to the virtual crack model and the distribution characteristics of opening displacement and cohesion as well as the experimental data of opening displacement, the distribution function of opening displacement was deduced, see [7-9]. Based on Westergard stress function, an analytical model of crack opening displacement has established, which can calculate the transfer loading between crack and solid [10]. There have been few studies on direct focus opening displacement. Most of researches calculated the size of FPZ by using the opening displacement as the intermediate parameter theory. In this process, the researchers had oversimplified the distribution of the opening displacement, even the opening displacement was taken as a linear distribution of the segment. Because of the inaccurate selection of the opening displacement distribution, the theoretical values were quite different from those ones determined by experiment. For this reason, it was necessary to further study the distribution characteristics of crack opening displacement of FPZ.

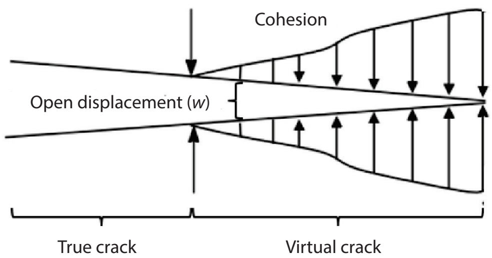

Figure 1. Diagram of crack opening displacement

Based on the DIC technology, the main target of the paper is to obtain the opening displacement value of FPZ by using the rectangular beam three-point bending beam specimen, and compared with the value obtained by the tradicional theoretical distribution function of opening displacement, to combine with the theory of damage mechanics [11, 12].

Theoretical analysis of crack opening displacement distribution function in FPZ

According to the virtual crack model, the opening displacement of FPZ is a parameter that reflects the opening degree of the virtual crack and the degree of damage in fracture ligament, fig. 1. It forms constitutive relation with the cohesion $\sigma(x)$. The cohesion is due to the bridging action of materials to prevent crack opening and propagation.

Based on the virtual crack model, the opening displacement $w(x)$ of FPZ is expressed as a dimensionless Taylor power series expansion [6-8], *e. g.*:

$$w(x) = \frac{4}{E\pi}\sum_{n=1}^{\infty} c_n \left(\frac{x}{b}\right)^n \tag{1}$$

where $w(x)$ is the opening displacement of FPZ, x – the distance from the initial crack tip, b – the length of the FPZ, E – the elastic modulus of the material, and c_n – the expansion type coefficient.

According to the boundary condition of the opening displacement, the opening displacement has a finite value at the front end and the rear end of FPZ, and there is constitutive relation between the opening displacement and the cohesion. The coefficient c_n can be got in the expansion equation, and then it can be generalized to obtain the distribution function of the opening displacement of FPZ, given [8]:

$$w(x)_i = \frac{8K_\text{I}}{3E}\sqrt{\frac{2b}{\pi}\left(\frac{x}{b}\right)^{3/2}} \qquad 0 \le x \le b \tag{2}$$

where K_I is a stress intensity factor.

The opening displacement of FPZ can be obtained by eq. (2), and it shows that the opening displacement is increasing steadily. It is known from the damage mechanics that FPZ will be damaged during the development process. Although the material damage has a certain trend as a whole, and the locality will be random, which indicates that the opening displacement is unlikely to grow steadily. It has been shown that for the quasi-brittle materials, and the generation of FPZ during loading is due to the initiation and propagation of micro-cracks [2, 4, 5]. It is also the same with the large rock mass in field, where the fracture evolution modes in very complex condition have been revealed in [13].

The FPZ is not in the linear elastic state, which belongs to the category of damage mechanics. However, eq. (2) still contains the elastic modulus, *E*, which is a defect of this formula, and this will be further proved by the experimental data. Based on the analysis and comparison of the classical damage models, it can be seen that most of the damage models take strain as the basic parameter to measure the damage degree, but in term of the definition of strain, it reflects the deformation of region, no matter how small the region tends to be. In addition, the strain obtained is based on the deformation of the area of several or even tens of times the size of rock mineral particles, so it cannot accurately reflect the damage state of materials. The damage of rock is based on the separation of mineral particles and cements and the translation or rotation of particles, so the displacement of rock particles is the basic basis for describing damage. For this reason, a new fluctuation coefficient, λ_i, is defined in this paper, which describes the damage of rock. It is based on the variance of several displacement data points around the crack tip, and the length of the area covered by the data points should be larger than the maximum diameter of rock particles. The data points do not all fall on the same rock particle, and can reflect the displacement between different particles. The difference can better describe the damage characteristics. The area length should not exceed twice the maximum diameter, because the diameter of rock particles varies greatly. If the data points fall on smaller rock particles, these data points will contain more rock particles. Because of the disordered movement of particles, the variance obtained will be larger and the damage degree will be enlarged artificially. The specific formula can be given [4]:

$$\lambda_i = \sum_{n=i-2}^{i+2} \left(u_n - u\right)^2 \tag{3}$$

where λ_i is the represents the fluctuation coefficient of the horizontal displacement of the data point i, u_{n} – the horizontal displacement value of the nth data point, u – the average of five consecutive horizontal displacement values, and n – the horizontal displacement sequence value of the data point.

The expression of the horizontal elastic modulus damage factor describing the damage condition of rock is defined, and the anisotropy of rock properties can be written:

$$D_h(x) = \begin{cases} 0 & \lambda(x) < \lambda_e \\ 1 - \dfrac{\lambda(x) - \lambda_e}{\lambda(x)} & \lambda(x) \geq \lambda_e \end{cases} \tag{4}$$

where λ_{e} is the fluctuation coefficient of the horizontal displacement of the micro-view under the elastic condition, and $\lambda(x)$ is the distribution function of the horizontal displacement fluctuation coefficient of the micro-view.

Considering that the damage factor of horizontal modulus of elasticity contains fluctuation coefficient which represents the damage situation of the region with length, *s*, the theoretical value may reflect the delay effect of the experimental value. Therefore, the delay effect needs to be eliminated in the revised function, so the revised opening displacement distribution function can be suggested:

$$w(x)_r = \frac{8K_I}{3ED_h(x)}\sqrt{\frac{2b}{\pi}}\left(\frac{x-s/2}{b}\right)^{3/2} \qquad 0 \le x \le b \tag{5}$$

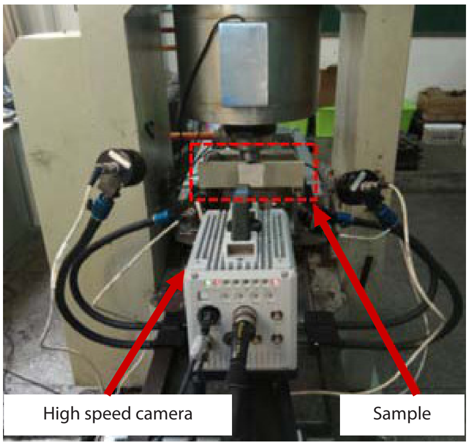

Figure 2. Photos of specimen loading

Experimental process and test results

Experimental process

The specimens are made of sandstone square beams with central pre-cracks, the three-point bending beam loading method is shown in fig. 2. The dimensional parameters of the specimens are in accordance with the standards testing method of International Society for Rock Mechanics and Rock Engineering). The specific design dimensions of the specimen are such as, the length L = 300 mm, the height H = 70 mm, the thickness B = 30 mm, and the crack length is 26.25 mm. The specific dimensional parameters of the actual processed specimens are shown in tab. 1.

Table 1. Dimensions of specimens

	CN-1	CN-2	CN-3	CN-4 N-1 N-2 N-3
Length, L [mm]	300.25	299.90	300.22	300.18 300.12 299.86 300.04
Height, H [mm]	69.00	69.20	69.80	70.00 70.03 69.58 69.94
Thickness, B [mm]	30.73	29.87	30.32	30.50 30.13 30.07 29.65
Crack length, α [mm]	26.50	25.80	27.50	26.20 0 0 0

The loading span, S, of the three-point bending beam specimen is 280 mm. In the process of making pre-cracks, in order to reduce the damage and avoid the error caused by the manual processing of cracks, the wire cutter is used to make the crack. The crack width is 0.3 mm, which made by a 0.2 mm diameter diamond wire. Other specific dimensions are shown in tab. 1. The dimensional parameters in tab. 1 are the average of the test results for different specimens. Image acquisition with high-speed camera, effective pixel is 2048 × 2048, equipped with 100 mm fixed-focus lens. The image acquisition rate is one for each 0.001 mm change of the center deflection of the specimen and LED white light source is placed on both sides of the camera. The experimental loading system is RMT-150B. In order to stably control the whole process of specimen loading, the vertical deflection sensor is used to measure the intermediate deflection of the beam as a servo feedback signal with a control rate of 0.0002 mm/s.

Analysis of the opening displacement distribution function of the damage

Acquisition of elastic modulus damage factor distribution function

By matching the image before deformation and the image at the peak, the horizontal displacement of the observation area can be obtained at the peak. Taking the CN-2 specimen as an example to obtain the horizontal displacement of FPZ, the front end of FPZ is marked as the zero point. Three vertical sampling lines with length of 15 mm are placed on the horizontal conur map, and are located on the extension-line of the pre-cracked center line (H_2) and 0.4 mm around H_2 (H_1, H_3) as shown in fig. 3. It can be seen from the literature [4] that the three sampling lines are evenly distributed within the width boundary of FPZ, which ensure the comprehensiveness and accuracy of the obtained data, this can also better reflect the experimental phenomenon-, and the length of the sampling line is greater than the length of FPZ.

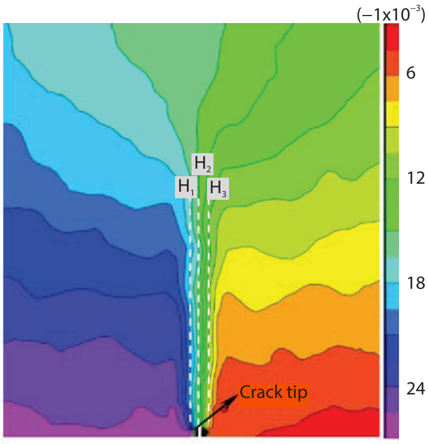

Figure 3. Sampling lines (H_1-H_3)

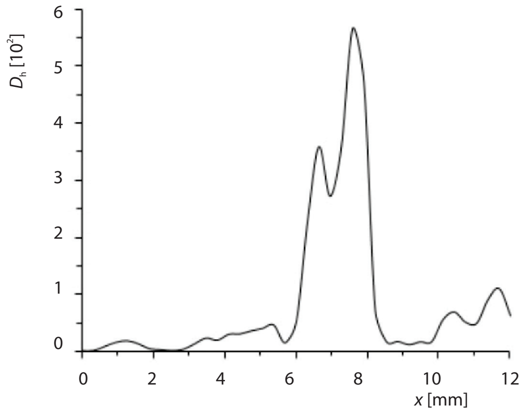

Figure 4. Horizontal elastic modulus damage factor

The horizontal displacement value on the sampling line is obtained by the VIC-2D software. In order to make the data better represent the deformation of FPZ, the horizontal displacements obtained by the three sampling lines are averaged, and then the mean value is brought into formula (3) obtains the fluctuation coefficient of the micro-view. Reference to the [4], the fluctuation coefficient of the linear elastic region $\lambda_e = 5.38 \cdot 10^{-8}$ is obtained. The $\lambda(x)$ is obtained though fitting the wave coefficients of FPZ by ORIGIN software. Then brings λ_e, $\lambda(x)$ into formula (4) obtain the horizontal elastic modulus damage factor distribution function. The function curve is shown in fig. 4. The horizontal x-axis represents the position of the horizontal elastic modulus damage factor. The vertical y-axis represents the horizontal elastic modulus damage factor. It can be seen from the figure that the horizontal damage factor in the interval of 6~8 mm is larger than that near the prefabricated crack tip due to local data anomalies or rock heterogeneity. Excluding this part, after calculating the theoretical value of the revised opening displacement distribution function, the theoretical value of the opening displacement of this part is calculated by function interpolation. It can be seen from the figure that the internal damage of the whole FPZ is non-uniform. Overall, the damage degree from the front end to the rear end of FPZ increases non-linearly and the damage at the rear end of FPZ is serious.

Experimental values of opening displacement

Based on the horizontal displacement conur map of the CN-2 specimen, the sampling lines H_4 and H_5 are made at the position that have 0.8 mm away from the center line of the prefabricated crack, as shown in fig. 5.

The curve of the opening displacement distribution is shown in fig. 6. The horizontal x-axis represents the position of the horizontal opening displacement, and the vertical y-axis represents the opening displacement. It can be seen from fig. 6 that the opening displacement

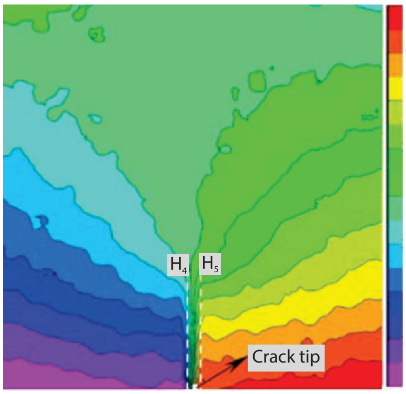

Figure 5. Sampling line (H_4, H_5)

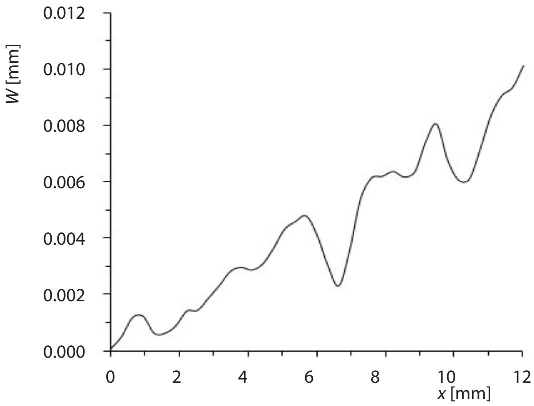

Figure 6. Distribution curves of the opening displacement

value of the front end portion the rear end portion of FPZ fluctuates and reaches the maximum value near the rear end portion, which further verifies the non-uniformity of the damage of FPZ, and the damage at the rear end portion is the most serious.

Comparison of theoretical and experimental values

This study only verifies whether the overall and local trends of the theoretical and experimental values of the formula function are close. The theoretical values are calculated by:

$$w(x)_i \propto \left(\frac{x}{b}\right)^{3/2} \quad 0 \le x \le b \tag{6}$$

$$w(x)_r \propto \frac{1}{D_h(x)}\left(\frac{x - s/2}{b}\right)^{3/2} \quad 0 \le x \le b \tag{7}$$

where the length of FPZ of the specimen is 12 mm, and b is equal to 12. However, in order to facilitate comparison of theoretical and experimental values, the theoretical values will be unified.

In order to obtain the horizontal displacement value, two sampling lines H_4 and H_5 are adopted. The initial opening displacement is obtained by subtracting the horizontal displacement of sampling line H_4 from the sampling line H_5. This initial opening displacement is not accurate because the value contains the displacement value due to the elastic deformation of the material. However, the definition of the opening displacement in the virtual crack model is the pure opening displacement of the virtual crack, so it is necessary to subtract the displacement value due to the elastic deformation. The calculation formula can be expressed:

$$w(x) = w(x)_0 - \varepsilon_f L \tag{8}$$

where $w(x)_0$ is the initial opening displacement, ε_f – the ultimate tensile strain, which is obtained by the aforementioned non-grooved three-point bending beam, and L – the horizontal distance of the sampling line, which is equal to 1.6 mm. The range of rock particle diameters measured in conjunction with the experiments herein is from 0.15-0.7 mm, and the distance between the data points is 0.3233 mm, as five data points are taken, and the length ranges from 1.27 mm.

The experimental value curve, the theoretical opening displacement value curve w_i, and the revised theoretical opening displacement curve w_r are shown in fig. 7, and x represents the ordinate value of the position where the displacement value is located. It can be seen from fig. 8 that the theoretical value can reflect the overall growth trend of the experimental value, but since FPZ is damaged state, the experimental value locally has fluctuations, and the traditional theoretical value cannot reflect this phenomenon.

It can be seen from fig. 7 that the revised opening displacement can reflect not only the overall growth trend of the opening displacement, but also can reflect the local fluctuation characteristics of the experimental values. Through the peak or valley value of the local fluctuation of the region, it is found that the revised theoretical fluctuation value is not completely consistent with the experimental value, because the fluctuation coefficient, λ, is obtained based on the average of the horizontal displacement from five data points around it. The damage situation reflected by this variance value is different from the damage situation of a certain data point. In theory, it is possible to ensure that the variance value is more accurate by narrowing the local length covered by the data points, but this method has a certain limitation because it is affected by the minimum diameter of the rock particles (the smallest particle of the rock observed by the microscope is 0.15 mm). Once the data point length is less than the minimum value of the particle diameter, the variance value will mostly be close to zero, because the data points are all located on the same rock particle, and their displacement values are basically the same.

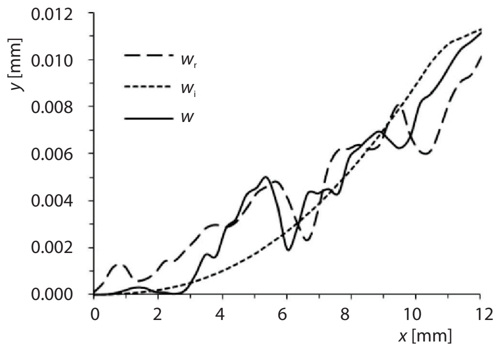

Figure 7. Comparison of theoretical and experimental values of opening displacement

Conclusion

The original displacement value of the FPZ was obtained by the DIC technology. The opening displacement was given in the experiment. Due to large number of random micro-cracks of FPZ. The displacement between particles is in disordered fluctuation state, so the damage is non-linear, but the damage at the back end of FPZ is serious overall. The fluctuation coefficient indicates the disordered degree of displacement, which can better reflect the damage state of FPZ. In order to get the true experimental value of the opening displacement of FPZ, The limit elastic strain of the sampling line area should be removed. The opening displacement increases from the front to the back end of FPZ as a whole, due to the non-linearity of the damage, the local opening displacement shows fluctuating state. The elastic modulus has been always taken as a fixed value for the traditional opening displacement distribution function of virtual crack, and the material damage is not considered, so the theoretical value obtained is greatly deviated from the experimental value. By introducing the damage factor to weaken the elastic modulus of the FPZ, the crack opening displacement distribution function is revised, and the theoretical calculation value will be closer to the experimental test results.

Acknowledgment

The research was financially supported by the National Key Research and Development Program of China (No. 2016YFC0600701), and National Natural Science Foundation of China (No. 51674101, 5147422). Key Laboratory Open Project Fund in Henan Province (No. S201605).

References

[1] Lin, Q., *et al*., Opening and Mixed-Mode Fracture Initiation in a Quasi-Brittle Material, *Journal of Engineering Mechanics*, *139* (2012), 3, pp. 177-187
[2] Lin, Q., *et al*., Opening and Mixed Mode Fracture Processes in a Quasi-Brittle Material Via Digital Imaging, *Engineering Fracture Mechanics*, *131* (2014), 2, pp. 176-193
[3] Ji, W. W., *et al*., Fracture Characteristics of Two Types of Rocks Based on Digital Image Correlation, *Chinese Journal of Rock Mechanics and Engineering*, *37* (2016), 8, pp. 2299-2305
[4] Qiao, Y., *et al*., Test Method of Determination of Rock Fracture Process Zone, *Journal of Experimental Mechanics*, *34* (2019), 2, pp. 1-13
[5] Nathan, D., *et al*., On the Link between Fracture Toughness, Tensile Strength, and Fracture Process Zone in Anisotropic Rocks, *Engineering Fracture Mechanics*, *201* (2018), 1, pp. 56-79
[6] Qing, L. B., *et al*., Study of Concrete Fracture Process Zone Based on Fictitious Crack Model, *Engineering Mechanics*, *29* (2012), 9, pp. 112-116
[7] Wang, L. M., *et al*., Singularity of Crack Cohesive Stress Distribution along the Fracture Process Zone of Concrete, *Chinese Journal of Applied Mechanics*, *21* (2004), 1, pp. 30-35
[8] Wang, L. M., *et al*., Analysis on Cohesive Crack Opening Displacement Considering the Strain Softening Effect, Science in China, *49* (2006), 1, pp. 88-101
[9] Wang, L. M., *et al*., Calculation and Experiment on Cohesive Resistance Crack of Quasi-Brittle Materials, *Chinese Quarterly of Mechanics*, *34* (2013), 3, pp. 456-462
[10] Wang, W. D., *et al*., Analytical Solutions for Crack Opening Displacements of Eccentric Cracks in Thin-Walled Metallic Plates, *Thin-Walled Structures*, *123* (2018), 2, pp. 371-381
[11] Zhu, S. Y., *et al*., Thermally Induced Variation of Primary Wave Velocity in Granite From Yantai: Experimental and Modelling Results, *International Journal of Thermal Sciences*, *114* (2017), 4, pp. 320-326
[12] Lei, G., *et al*., The Convective Heat Transfer of Fractal Porous Media Under Stress Condition, *International Journal of Thermal Sciences*, *137* (2019), 1, pp. 55-63
[13] Gao, M. Z., *et al*., Field Experiments on Fracture Evolution and Correlations between Connectivity and Abutment Pressure Under Top Coal Caving Conditions, *International Journal of Rock Mechanics and Mining Science*, *111* (2018), Nov., pp. 84-93

Paper submitted: September 13, 2018
Paper revised: November 11, 2018
Paper accepted: December 20, 2018